J Mater Sci (2007) 42:8298–8305
DOI 10.1007/s10853-007-1504-2

The effect of manganese on the microstructure and mechanical properties of zinc–aluminium based ZA-8 alloy

Ahmet Türk · Mehmet Durman · E. Sabri Kayali

Received: 28 February 2006 / Accepted: 5 January 2007 / Published online: 9 June 2007

Abstract In this investigation, the effect of manganese as an alloying element in the range 0.01%–0.53 wt.%, on the hardness, 0.2% yield, tensile and impact strength, and creep properties of a gravity cast Zn–Al based ZA-8 alloy has been investigated. It was found that addition of Mn over the entire range of concentrations has a useful effect on the hardness of the alloy. Also, the 0.2% yield and ultimate tensile strength (UTS) of the samples did not change significantly with Mn additions up to 0.045 wt.% but decreased with a further increase in Mn content. Furthermore, the impact strength of the alloy improved with increasing Mn up to 0.045 wt.% and then decreased gradually with a further increase in Mn content. On the other hand, the creep resistance of the alloy increased continuously with increasing Mn content up to 0.53 wt.% Mn. Metallographic studies showed that addition of Mn resulted in microstructural modifications of the alloy involving the formation of complex intermetallic compound identified as $MnAl_6$. The increase in creep resistance and decrease in tensile and impact strength were thought to have been caused by the changing morphology and amount of the intermetallic.

A. Türk (✉) · M. Durman
Department of Metallurgical and Materials Engineering, Sakarya University, Esentepe Campus, 54187 Adapazari, Turkey
e-mail: aturk@sakarya.edu.tr

E. S. Kayali
Department of Metallurgical and Materials Engineering, Istanbul Technical University, 80626 Istanbul, Turkey

Introduction

The major advancement in the zinc industry over the past years has been the development of zinc alloys with higher aluminium contents, namely ZA-8 (Zn–8%Al–1% Cu–0.03% Mg), ZA-12 (Zn–11%Al–1%Cu–0.03%Mg) and ZA-27 (Zn–27%Al–2%Cu–0.02%Mg), known as ZA alloys to supplement the well-established No.3 (Zn–4% Al–0.05%Mg) and No.5 (Zn–4%Al–1% Cu–0.05%Mg) alloys used in pressure die-casting [1–3]. These new zinc–aluminium based alloys have high strength and hardness, improved creep and wear resistance and lower density, and, although developed originally for sand and gravity casting, they are now being used in growing amounts for pressure die casting [4–9]. These alloys, which possess excellent casting and mechanical properties, have been increasingly used to replace traditional alloys such as aluminium, bronze, brass and cast iron in many industrial applications [10, 11].

More recently, some investigators [12–21] have determined the mechanical properties of these alloys in gravity cast and pressure die-cast form at room temperature and elevated temperatures. Though it has been shown that alloy ZA-8 has considerably better overall creep performance than the Zamak alloys and the others in the family of ZA alloys [12, 13, 22]. This alloy has still found limited applications involving high stress conditions due to its lower creep resistance, compared to traditional aluminium alloys and other structural materials, especially at temperatures above 100 °C. This has resulted in a major loss of market potential for this alloy; otherwise it is an excellent material. It has been suggested that this problem could be reduced through alloying with different elements [14, 23–27] or dispersing hard second particles in the alloy matrix [28–32]. Cu and Mg are added to the Zn–Al based alloys to

improve the mechanical properties. The Mg additions used in these alloys, which are usually in the range 0.01–0.03 wt.%, increase the hardness, tensile strength and intergranular corrosion resistance of these alloys [1, 33]. The Cu content used in these alloys, typically in the range 1–2.5 wt.%, also increase the hardness, tensile strength and creep resistance of these materials [14, 33, 34]. There has been some research [15, 35–38] into the effects of Si, Mn, Ni and Ti alloying element additions on the mechanical properties and wear characteristic of Zn–Al based alloys. However, very few data are available in the literature on the effect of manganese on the microstructure and mechanical properties of these alloys [38].

In view of the above, purpose of this research was to examine the effect of Mn in the range from 0.01% to 0.53 wt.% on the mechanical properties and the microstructure of the gravity-cast Zn–Al based ZA-8 alloy.

Experimental details

Casting of alloys

The alloys were prepared by liquid metallurgy route in a permanent cast iron mould in the form of cylindrical castings (size: 16 mm in diameter, 150 mm long). An electrical furnace was used at the first stage for melting the Al in a graphite crucible under a nitrogen protective atmosphere. After melting the Al, the melt temperature was increased to 750 °C and then Al–Cu and Al–Mn master alloys were introduced to the melt. Subsequently, Zn was added and the melt temperature was decreased to 650 °C. At final stage, pure magnesium (99.99 wt.%) was added to the melt at about 600–620 °C with vigorous stirring under protective gas. The melts were then poured into permanent cast iron mould pre-heated to about 200 °C. The raw materials were commercially pure Al (99.8 wt.%), Zn (99.95 wt.%), Al–Cu master alloy (50 wt.% Cu) and Al–Mn master alloy (10 wt.% Mn). Thus, eleven different Zn–Al-based alloys containing Mn up to 0.53 wt.% were prepared. The chemical compositions of the alloys determined by atomic absorption spectroscopy are presented in Table 1.

Mechanical tests

Brinell hardness tests of the alloys were performed on ground and polished samples using a ball diameter of 2.5 mm under an applied load 187.5 kg for 30 s. At least 10 impressions were made to determine the mean value of the hardness at different locations to circumvent the possible effect of any alloying element segregation.

Tensile tests were carried out on 6 mm gauge diameter, 25 mm gauge length specimens at the strain rate of $0.002\ s^{-1}$ using a Lloyd T50K universal tensile testing machine. Charpy impact tests were conducted using standard unnotched impact samples having the dimensions of $10 \times 10 \times 55\ mm^3$ prepared in accordance with ASTM E 23 using a charpy impact testing machine. All the tests were conducted on three samples for each alloy, and the average value was considered.

Round tensile specimens machined from the cast bars in accordance with ASTM E 8 having a cross sectional area of about 30 mm^2 and a gauge length of 25 mm were used for creep testing. Creep tests were performed using a standard lever arm creep testing machine, details of which are reported elsewhere [14]. Creep tests were continued until a well defined secondary creep region was obtained. Curves of creep elongation versus time were recorded in the each test. From the plots, secondary creep rate and time to 1% creep strain were computed. All the tests were carried out at a constant load of 40 MPa at 120 °C. Each test was repeated three times, and the average value considered.

Metallography

Microstructural examination of the experimental alloys was conventionally carried out on ground and polished samples using optical microscope. The etching agent used was 2 % Nital. A JEOL JSM T320 scanning electron microscope (SEM) was also used for detailed microstructural studies. SEM investigation was made in the as-polished samples using a large-area backscattered electron detector to produce an image. The large atomic number differences between the Al-rich and Zn-rich phases allowed the production of medium-resolution images of good contrast in this alloy which displayed the larger scale features of the structure very well. Fracture surfaces of typical samples subjected to tensile and impact tests were investigated using the SEM. X-ray diffraction analysis was also carried out to identify the phases present in the experimental alloys using a Rigaku D-Max 1000 X-ray difractometer with Co Kα radiation.

Results

Microstructure

The as-cast structure of the ZA-8 alloy without Mn is shown in the optical micrograph of Fig. 1. The general view in this figure showed a microstructure which was heterogeneous and consisted of numerous relatively well

Table 1 Chemical composition of the experimental alloys (wt. %)

Alloys	Al	Cu	Mg	Mn	Zn
ZA-8 (Std.)	7.95	0.97	0.032	–	Balance
ZA/1	8.10	1.00	0.026	0.010	Balance
ZA/2	8.05	1.00	0.026	0.026	Balance
ZA/3	8.05	1.02	0.026	0.045	Balance
ZA/4	8.02	1.04	0.026	0.063	Balance
ZA/5	8.10	1.06	0.026	0.090	Balance
ZA/6	8.06	1.02	0.026	0.140	Balance
ZA/7	8.16	1.00	0.026	0.174	Balance
ZA/8	8.20	1.07	0.026	0.220	Balance
ZA/9	8.15	1.10	0.026	0.300	Balance
ZA/10	8.20	1.08	0.026	0.530	Balance

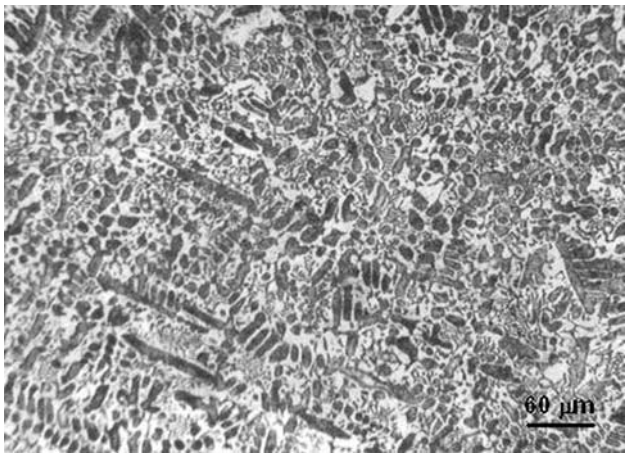

Fig. 1 Optical micrograph of Standard ZA-8 alloy without Mn

developed primary β dendrites in a lamellar eutectic (α+η) matrix. The β phase, which is unstable below 275 °C, had decomposed to form zinc-rich η and aluminium-rich α equilibrium phases in accordance with eutectoid reaction in Zn–Al binary phase diagram.

Figure 2a–d shows the optical microstructures of typical Mn containing zinc alloys ZA/3 (0.045% Mn), ZA/8 (0.22% Mn), ZA/9 (0.30% Mn) and ZA/10 (0.53% Mn) alloys, respectively. The presence of Mn in the alloy resulted in modifying its basic as-cast structure in terms of reducing the size of β dendrites and increasing the amount of eutectic phase in a more regular form and, also produced finer eutectic in ZA-8 matrix (Fig. 2a–c). As can be seen from Fig. 2c and d, this element formed a complex intermetallic compound with an angular morphology in the alloys containing high amounts of Mn.

Figure 3 shows the scanning electron micrographs of the as cast alloys, for different manganese concentrations. The microstructure of alloy with 0.01 wt.% Mn represents primary β dendrite surrounded lamellar eutectic structure (Fig. 3a). The SEM image of the alloy ZA/2 containing 0.026 wt.% Mn is presented at high magnification in Fig. 3b. From here, the effect of Mn on the microstructure of the alloy system was clearly observed. The addition of Mn to the alloy had a nucleating effect of the primary β dendrites phase and also formed small, fine and irregularly-shaped intermetallic compound in the dendrites and eutectic regions. Figures 3c and d show SEM micrographs of ZA/5 and ZA/10 alloys containing 0.09 wt.% Mn and 0.53 wt.% Mn, respectively, at high magnifications. It was observed from these figures that increasing manganese content in the alloy affected the amount and distribution of intermetallic particles in the matrix wherein the number and size of particles increased.

The X-ray spectra of the ZA/10 alloy containing 0.53 wt.% Mn is shown in Fig. 4. The diffraction showed peaks corresponding to those of the zinc-rich and aluminium-rich phases of the binary Zn–Al system and small peaks identified as $MnAl_6$ phase.

Mechanical properties

Average values obtained from the mechanical tests of the experimental alloys containing in the range 0.01–0.53 wt.% Mn are listed in Table 2. The variation of hardness, 0.2% yield strength, UTS, impact strength, secondary creep rate, and time to 1% creep strain of the alloys with Mn content are shown in Figs. 5–7, respectively.

It can be seen from Fig. 5 that addition of Mn to the alloy system marginally reduced hardness initially and then tended to increase, attain the peak, finally showing a reduction in hardness with increasing Mn content. 0.2% Yield strength followed a practically reverse trend. Figure 6 represents the tensile and impact strength of the experimental alloys as a function of the manganese content. The tensile and impact strength of the ZA-8 alloy

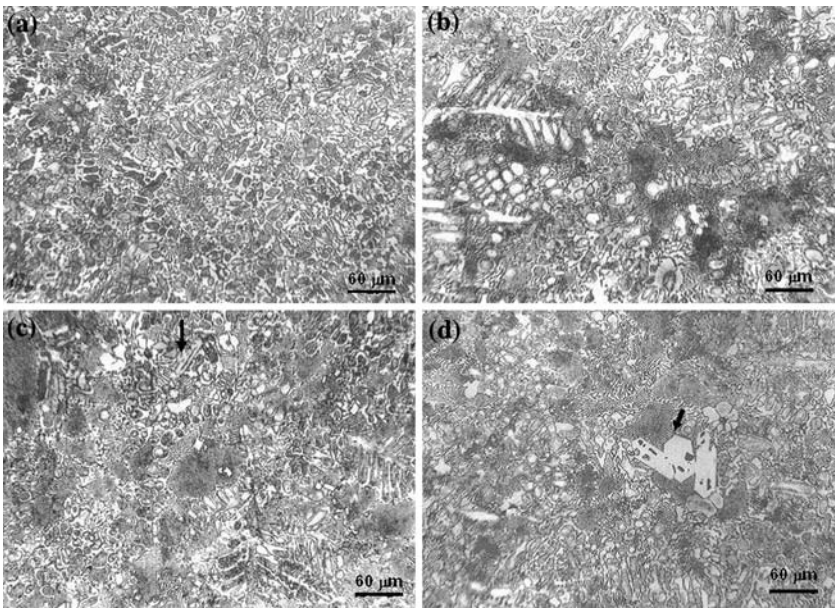

Fig. 2 Optical micrographs of as cast ZA-8 alloys with different wt.% Mn: (**a**) 0.045, (**b**) 0.22, (**c**) 0.30 and (**d**) 0.53

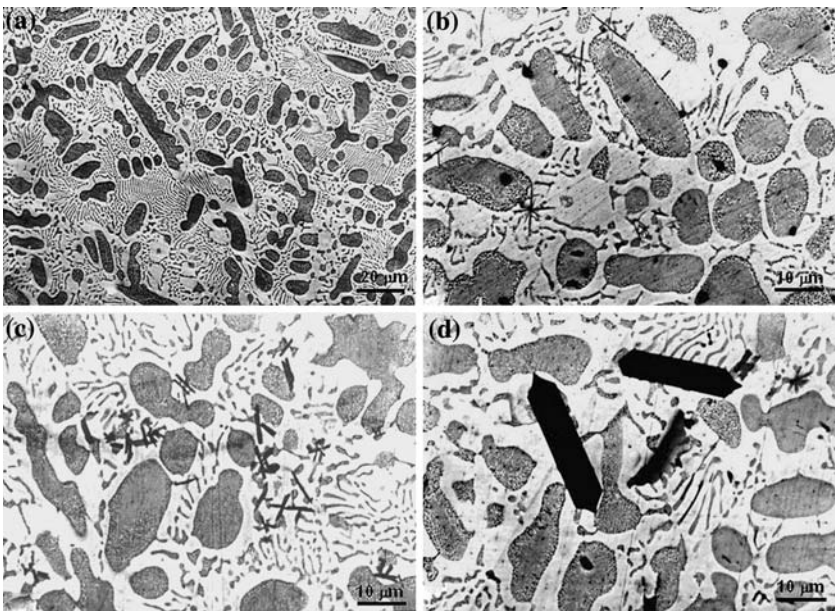

Fig. 3 SEM micrographs of as cast ZA-8 alloys with different wt.% Mn: (**a**) 0.026, (**b**) 0.09 and (**c**) 0.53

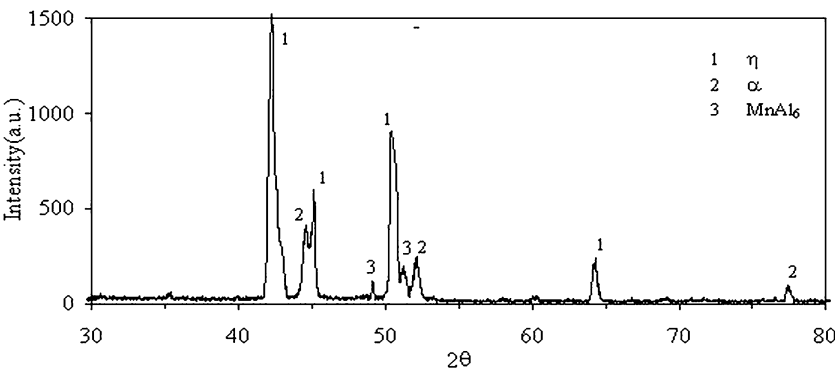

Fig. 4 X-ray spectra of ZA/10 alloy

Table 2 The mechanical properties of the experimental alloys

Alloys	Hardness (BHN)	0.2% Yield strength	UTS (MPa)	Impact strength (J)	Creep Rate ($\times 10^{-7}$/s)	Time to 1% Creep Strain(ks)
Std. ZA-8	108	279	300	36	1.453	55.44
ZA/1	107	288	306	38	1.430	56.88
ZA/2	108	290	305	39	1.250	63.00
ZA/3	110	292	309	45	1.165	68.40
ZA/4	110	276	295	32	0.909	88.20
ZA/5	111	273	291	10	0.890	90.90
ZA/6	111	267	283	9	0.870	95.40
ZA/7	111	255	266	10	0.874	93.60
ZA/8	112	251	260	9	0.802	97.56
ZA/9	111	243	250	7	0.767	106.2
ZA/10	111	241	248	6	0.589	122.4

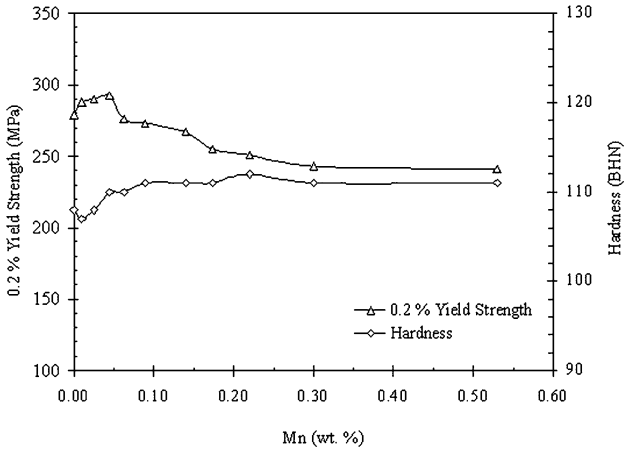

Fig. 5 Hardness and 0.2% yield strength of the alloys as a function of manganese content

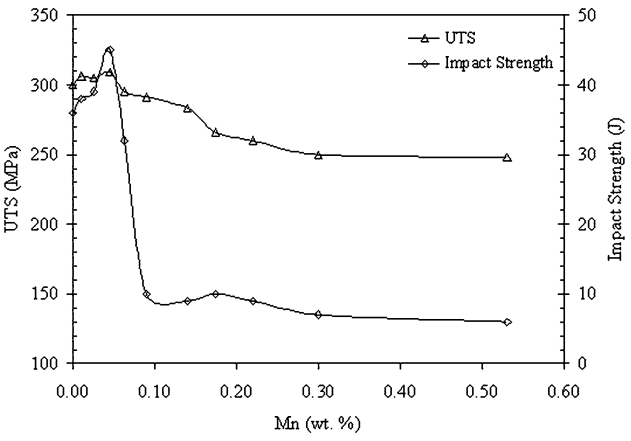

Fig. 6 Tensile and Impact strength of the alloys as a function of manganese content

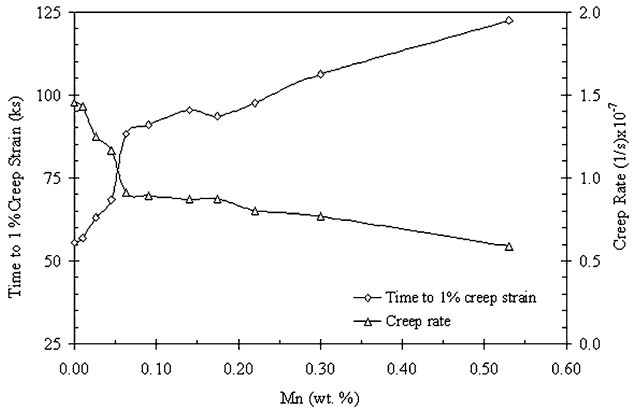

Fig. 7 Secondary creep rate and time to 1% creep strain as a function of Mn content

improved with increasing Mn up to 0.045 wt.% and then reduced gradually with a further increase in Mn concentration.

Creep properties of the experimental alloys as a function of Mn content have been plotted in Fig. 7. It was noticed that secondary creep rate and time to 1% creep strain of the standard ZA-8 alloy obtained as $1.453 \times 10^{-7}\ s^{-1}$ and 55.44 ks, respectively. It can be seen from Fig. 7, the secondary creep rate of the alloys continuously decreased with increasing Mn addition and minimum creep rate in the investigated alloys was obtained for the alloy ZA/10 containing 0.53 wt.% Mn. The average of creep rate in this alloy is $0.589 \times 10^{-7}\ s^{-1}$.

Time to 1% creep strain of the standard alloy continuously increased with the increasing addition of manganese. It may also be noted that the alloy ZA/10 containing 0.53 wt.% Mn showed maximum value of creep strength

(expressed as time to obtain 1% total creep strain). This average value (122.4 ks) is 120% improvement over the one without Mn.

Fracture surfaces

Fractographic features of the experimental alloys after tensile and impact tests can be seen in Fig. 8. Figure 8a and b represent tensile test fracture surface of the standard alloy without Mn and ZA/10 alloy containing 0.53 wt.% Mn. The alloy containing 0.53 wt.% Mn showed a mixed mode of fracture exhibiting ductile and brittle failure while ZA-8 alloy showed ductile fracture. The alloy also showed minimum value of tensile strength that 20 % less than the one without Mn (Fig. 6).

The impact test fracture surfaces of the alloy ZA-8, ZA/3 and ZA/10 are given in Fig. 8c–e, respectively. Standard ZA-8 alloy showed ductile and brittle fracture failure in the fracture surface (Fig. 8c). Fracture surface of alloy ZA/3 shows the presence of more dimples indicating the occurrence of ductile mode of fracture (Fig. 8d). The impact strength of this alloy was the maximum i.e. 45 J. Increasing manganese content significantly affected the fracture surface of the alloys. In this context, alloy ZA/10 containing 0.53 wt.% Mn showed brittle rupture and less ductile failure with dimples, as shown in Fig. 8e as compared to Fig. 8d; minimum impact strength (6 J) in the alloys was obtained for this alloy (Fig. 6).

Discussion

Microstructure

Manganese has a solubility in zinc up to 0.47 wt.% at 400 °C which falls to a very small value at room temperature, when the zinc is alloyed with aluminium, this limited solubility for manganese is reduced even further [33]. The solid solubility values of 0.0006 wt.% Mn at 390 °C and 0.0013 wt.% Mn at 420 °C have been reported for die casting Zamak alloys. Therefore, addition of 0.5 wt.% Mn to the Zn–Al alloys formed intermetallic compound with aluminium [39] and also caused fine grained and strong microstructure [33]. L'Esperance et al. [40] have reported that intermetallic particles were in the forms of Al_3Mn and Al_6Mn in creep resistant Zn–Al based alloy (ZATEC) containing 0.03 wt.% Mn. On the other hand, it has been suggested by Yuanyuan and co-workers [35] that addition

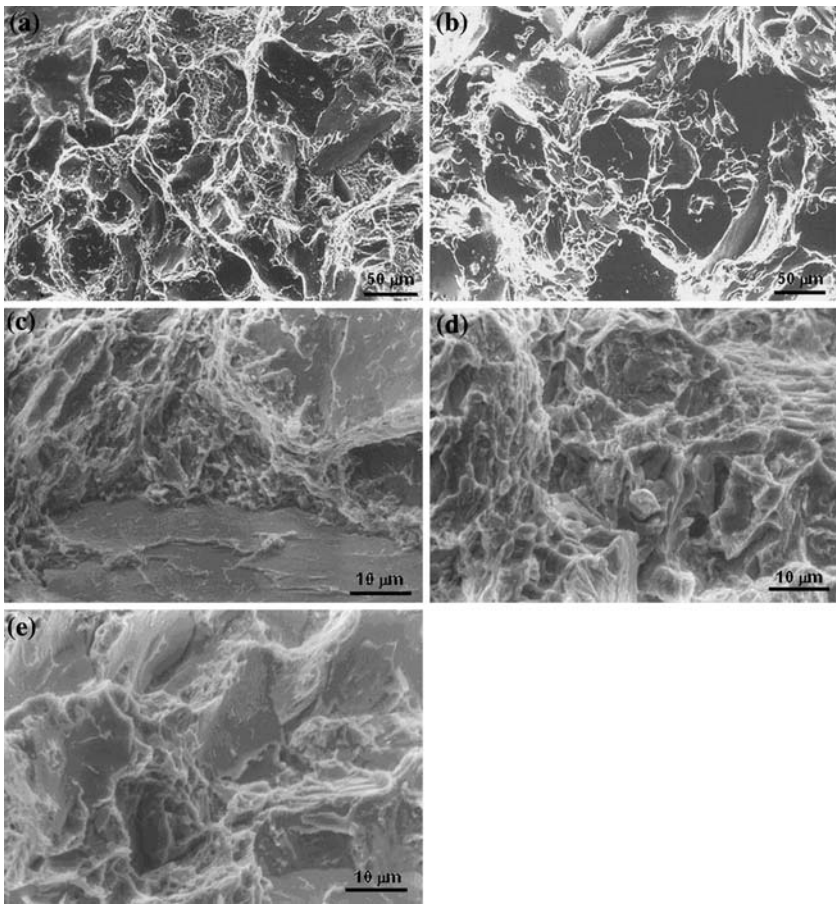

Fig. 8 Tensile test fracture surface of (**a**) Standard ZA-8 and (**b**) ZA/10 alloys, and Impact test fracture surfaces of (**c**) ZA-8, (**d**) ZA/3 and (**e**) ZA/10 alloys, respectively

of Mn to ZA-27 alloy in the range 0.18%–1.22 wt.% forms Al_5ZnMn ternary intermetallic particles and increases wear resistance and high temperature tensile strength. Ma et al. have stated [36] these Mn-rich intermetallics to appear in the microstructure of ZA-27 alloy when the Mn content exceeds 0.3 wt % and they reported that hardness of these particles was around 340 HV.

The results obtained from this investigation indicate that the grain structure of primary β phase in the microstructure of ZA-8 alloy can be modified by the addition of manganese in the range 0.01–0.53 wt.% (Figs. 1–2). Manganese caused grain refinement and increased the volume fraction of eutectic phase accompanied by a more regular form (Fig. 2). XRD analysis showed that the intermetallic compounds in the microstructure of ZA-8 alloy containing manganese were in the form of $MnAl_6$. This form of intermetallic was also reported by L'Esperance et al. [40]. Others who studied the effect of Mn on Zn–Al alloys reported the formation of Al_5ZnMn or binary Al_3Mn intermetallics [35]. In addition, these intermetallic compounds provide nucleation to primary β phase (Fig. 3b) and cause grain-refinement. Mn-rich intermetallic was observed in alloys containing above 0.010 wt.% Mn in the present study (Fig. 3a–b).

Mechanical properties

The improvement in creep resistance due to Mn addition was attributed to the formation of $MnAl_6$ intermetallic compound formed in the structure (Figs. 2–4) because stress and deformation rate in the creep test are lower than that of the tensile test. These Mn-rich intermetallics with complex shape (Figs. 2, 3) decreased the tensile and impact strength of the alloy (Fig. 6) due to stress concentration in the sharp corners, and also caused brittle rupture instead of ductile failure which was showed in the alloy containing small amount of Mn (Fig. 8). As can be seen in Fig. 8b and e, the tensile and impact fracture surfaces of the alloy containing high volume of Mn represented brittle failure due to these intermetallic particles. Manganese also increased the amount of the eutectic with more regular form in the alloys (Fig. 2). Thus, the regular lamellar eutectic morphology combined with quantity of $MnAl_6$ intemetallic compound in the structure was responsible for increasing the creep resistance of the alloys (Fig. 7). Similar observations have also been made elsewhere [34]. They reported that an increase volume fraction of eutectic structure of hyper eutectic Zn–Al alloys caused to decrease UTS and increase creep resistance.

As a result, it can be said that addition of Mn in the range from 0.045 wt.% to 0.063 wt.% to the ZA-8 alloy produce optimum mechanical properties at ambient and elevated temperature (Figs. 5–7). This Mn ratio increased creep strength of the standard alloy in the range 25–60% while hardness, 0.2% yield, tensile and impact strength were not affected significantly.

Conclusions

(1) The hardness value of the ZA-8 alloy containing Mn in the range 0.01 wt.% to 0.53 wt.% increased with Mn content. 0.2 % yield, tensile and impact strength of the alloy improved with increasing Mn up to 0.045 wt.% and then reduced gradually with a further increase in manganese ratio. The creep strength of ZA-8 alloy continuously increased with increasing manganese content in the investigated range and the highest value in the experimental alloys obtained in ratio of the 0.53 wt.% Mn. Optimum mechanical properties were achieved by addition of 0.045 wt.% to 0.063 wt.% Mn.

(2) Metallographic studies showed that Mn modifies the basic structure of standard ZA-8 alloy in terms of increasing the eutectic volume fraction and forming $MnAl_6$ intermetallic compound.

Acknowledgements The authors would like to thank the Scientific and Technical Research Council (TUBITAK) for financial support in this research.

References

1. Gervais E, Levert H, Bess M (1980) AFS Trans 88:183
2. Gervais E (1987) CIM Bull 80:67
3. Barnhurst RJ (1992) ASM Handbook, ASM International, vol 2. The Materials Information Society, Materials Park, OH, p 527
4. Gervais E, Barnhurst RJ, Loong CA (1985) J Metals 37:43
5. Barnhurst RJ (1988) SAE Trans 97(2):164
6. Gervais E, Lefebvre M, Loong CA (1985) SDCE 13th Int Die Cast Cong and Exp, Paper No G-T85-055, Milwaukee, WI, June 36, 1985, SDCD Inc, River Groove, USA
7. Pandey JP, Prasad BK (1998) Metall Mater Trans 29A:245
8. Prasad BK, Patwardhan AK, Yegneswaran AH (1996) Metall Mater Trans 27A:3513
9. Prasad BK, Patwardhan AK, Yegneswaran AH (1996) Wear 199:142
10. Kubel EJ (1987) Adv Metal Progress 7:51
11. Risdon TJ, Barnhurst RJ, Mihaichuk WM (1986) SAE Technical Paper, Int Cong and Exp, Detroit, Michigan, Paper No: 860064, Feb. 24-28, 1986
12. Durman M, Murphy S (1988) Z Metallkd 79:243
13. Durman M, Murphy S (1991) Z Metallkd 82:129
14. Türk A, Durman M, Kayali ES (1998) Z Metallkd 89:351
15. Akbulut H, Türk A (2000) Z Metallkd 91:436
16. Durman M (1998) Z Metallkd 89:417
17. Prasad BK (1996) Z Metallkd 87:226
18. Savaskan T, Aydin M, Odabasioglu HA (2001) Mater Sci Tech 17:681
19. Prasad BK, Yegneswaran AH, Patwardhan AK (1997) Z Metallkd 88:333

20. Savas MA, Altintas S (1992) J Mater Sci 28:1775
21. Anwar M, Murphy S (2001) J Mater Sci 36:411
22. Anwar M, Murphy S (2000) Mater Sci Tech 16:321
23. Savaskan T, Murphy S (1983) Z Metallkd 74:76
24. Prasad BK, Yegneswaran AH, Patwardhan AK (1996) J Mater Sci 31:6317
25. Prasad BK (2000) Mater Sci Eng A277:95
26. Türk A, Durman M, Kayali ES (2003) Z Metallkd 94:892
27. Prasad BK, Yegneswaran AH, Patwardhan AK (1998) J Mater Eng Perf 7:130
28. Dellis MA, Keustermans JP, Delannay F, Wegria J (1991) J Mater Sci Eng A135:253
29. Tao L, Dellis MA, Boland F, Delannay F, Wegria J (1995) Composites 26:611
30. El-Baradie ZM, Waly M, Abd El-Azim AN (2001) J Mater Proc Tech 114:194
31. Kurnaz SC (2003) Mater Sci Eng A346:108
32. Muthukumarasamy S, Seshan S (1995) Composites 26:387
33. Houghton ME, Murray MT (1984) Metals Forum 6:211
34. Türk A, Durman M, Kayali ES (2003) Z Metallkd 94:1001
35. Li Y, Ngai TL, Xia W, Zhang W (1996) Wear 198:129
36. Ma T, Chen QD, Li SC, Wang HM (1989) In: Ludema KC (ed) Proc Conf Wear Of Materials, Denver, Colorado, USA, 9–13 April, vol 1, ASME
37. Choudhury P, Das S, Datta BK (2002) J Mater Sci 37:2103
38. Dominguez C, Moreno Lopez MV, Rios-Jara D (2002) J Mater Sci 37:5123
39. Dale CH (1988) ASM Handbook, ASM International, vol 15. The Materials Information Society, Materials Park, OH, p 786
40. L'esperance G, Hong D, Gagne M, Barnhurst RJ (1993) Mater Sci Eng A172:1